

# A Different View of Solvent Effects in Crystallization

Han Wang <sup>1,2,†</sup>, Qiang Lin <sup>1,2,†</sup>, Xiangyu Dou <sup>1,2</sup>, Tao Yang <sup>1,2</sup> and Yongsheng Han <sup>1,\*</sup>

<sup>1</sup> State Key Laboratory of Multiphase Complex Systems, Institute of Process Engineering, Chinese Academy of Sciences, Beijing 100190, China; wanghan@ipe.ac.cn (H.W.); qlin@ipe.ac.cn (Q.L.); xydou@ipe.ac.cn (X.D.); tyang@ipe.ac.cn (T.Y.)

<sup>2</sup> University of Chinese Academy of Sciences, Beijing 100049, China

\* Correspondence: yshan@ipe.ac.cn; Tel.: +86-10-8254-5050

† The first two authors contributed equally.

Academic Editor: Shujun Zhang

Received: 2 November 2017; Accepted: 29 November 2017; Published: 3 December 2017

**Abstract:** Solvents are widely used in crystallization, but their effects on the shape development of crystals are under debate. Here, we report a view on how solvents play their role by considering the viscosity of solvents. We synthesize silver particles in a mixture of alcohol and water. The viscosity of the solvent is changed by varying the volume ratio of alcohol in water. With the variation of viscosity, diverse morphologies of silver particles are synthesized. Small cubic crystals are formed at low viscosity, while hierarchical flower-like particles are formed at high viscosity. Two alcohols are employed, namely ethanol and propanol. No matter which alcohol is employed, the results are similar. Due to the limitation of mass transfer at high viscosity, the particles synthesized in such solvent are smaller and stabilized by the solvent. When the solution containing these particles are dropped onto metal substrates, these tiny particles firstly aggregate, which is followed by classic crystallization, forming flower-like hierarchical structures. These findings show the importance of the viscosity of solvents in shaping particles, which is underestimated previously.

**Keywords:** crystallization; silver particles; solvent; diffusion; nanotechnology

## 1. Introduction

Diverse shapes of particles have various properties in catalysis [1–3], electronics [4–7] and molecular sensing [8–10], which is impressive when considering the carbon family, including carbon nanotubes, graphene, diamond, and so on. The control of the shape of particles is the big issue in the field of nanoscience, as well as being at the core of the emerging mesoscience [11]. Different approaches have been developed to control the shape of particles, including templating methods [12,13] and kinetic controlling methods [14,15]. When particles are synthesized in solution, the solvent is inevitable. The solvents include hydrophilic (such as water and ethanol) and hydrophobic chemicals (such as tetrachloromethane and bromobenzene). The effect of solvents on the structural evolution of particles has been widely investigated [16,17]. Different opinions have been proposed. Some researchers believe that the solvent molecules selectively adsorb on the crystallographic facets of crystals to hinder the growth of these facets [18], while other researchers believe that the solvent determines the solubility of the solute [19], which affects the supersaturation such that it influences the crystallization. High supersaturation is conducive to the formation of facets with high surface energy [20]. Here, we show a different view of the solvent effect in shaping particles from the perspective of chemical engineering.

Mass transfer is the basic issue of chemical engineering. It is also a dominant factor in the growth of particles [21,22]. Based on the theory of diffusion-limited aggregation, loose structures are normally formed under diffusion limitation [23]. By adjusting the chemical diffusion and reaction rates in calcium carbonate precipitation, we synthesized snow-shaped vaterite particles for the first time [24].

By delaying the feeding of reactants in the reduction of platinum, we synthesized dendritic platinum particles that deviated from the thermodynamic prediction [25]. Although the effect of chemical diffusion on particles is confirmed, the reasons why it influences the shape evolution of particles require further investigation.

In crystallization, the growth of particles follows one of two different pathways, namely classic crystallization and non-classic crystallization. Classic crystallization assumes a discrete nucleation followed by a growth via monomer addition, as was proposed by LaMer [26] and improved by Reiss [27], and has guided many syntheses [28,29]. Recently, substantial evidence has suggested that non-classic crystallization based on coalescence plays an important role in the growth of products [30,31]. Alivisatos et al. suggest that whether particles grow via the classic layer-wise pathway or the coalescence pathway is based on the nucleation period, and a long nucleation favors the coalescence growth pathway [32]. The nucleation process is dependent on the collision frequency of building blocks, which is influenced by the diffusion of chemicals. Therefore, the diffusivity of reactants may determine the growth pathway of particles, which is the main assumption we want to evaluate in this paper.

We employ the solution-based reduction approach to synthesize silver particles. The reduction of silver ions is carried out in a mixture of alcohol and water. The diffusion of chemicals is tuned by adjusting the viscosity of the solvent via changing the volume ratio of alcohol. The reduction of silver ions occurs in two kinds of solvents, namely ethanol-water and propanol-water mixtures. No matter which types of alcohol are used, the shapes of silver particles are similar at the similar diffusivity of silver ions. Small crystals are obtained at high diffusivity, while flower-like hierarchical structures are generated at low diffusivity of silver ions. Further investigation indicates that, at high diffusivity of the reactant, classic crystallization dominates the growth of particles, forming small crystals with a smooth surface. At low diffusivity, tiny crystals are formed in the solution. When the solution is dropped onto copper substrates, the tiny crystals firstly aggregate, which is followed by classic crystallization, forming flower-like hierarchical structures.

## 2. Results and Discussion

The silver particles synthesized in different alcohol volume ratios were characterized by electronic microscopy, as shown in Figure 1. The shapes of the particles were different at different alcohol volume ratios. The particles synthesized with 20 vol % ethanol have a defined geometrical shape and smooth surfaces (Figure 1A1). The transmission electron microscopy (TEM) image shows the twin crystallographic structure of these particles, as shown in Figure 1A2. The selected area electron diffraction (SAED) pattern in Figure 1A3 indicates single crystalline features with clear diffraction points. When the ethanol was increased to 50 vol %, the particles obtained showed a flower-like profile with rough surfaces. The low-magnification SEM image in Figure 1B1 indicates the uniform and large yield of this structure. The high-magnification image (Figure 1B2) reveals that these particles were built up by the interconnection of plates. The SAED pattern of these particles exhibited a ring-pattern, as shown in Figure 1B3, indicating their polycrystalline character. A great deal of work has proved that the formation of twinned planes is the result of the energy minimization of crystals [33]. The smooth surface of the small crystals indicates that selective deposition or surface reconstructing took place during crystallization, suggesting that the growth of small crystals was more likely to follow the classic layer-wise growth scenario, while the polycrystalline features of hierarchical structures indicates a different growth scenario. To discover the relationship between the shape of the particles and the diffusion rate of silver ions, the diffusivity of silver ions at various ratios of ethanol was quantified, as shown in Figure 2. Since the amount of ethanol influenced the reduction rate, the reaction rate of silver ions was also quantified, as shown in the inset of Figure 2. It was found that the reaction rates changed slightly, while the diffusivity of the silver ions decreased to approximately one third with an increase in volume ratio of ethanol from 0.2 to 0.5. When the diffusion of chemicals was reduced, both nucleation and growth of particles were impacted, which was likely responsible for the different

crystallization scenarios. Hence, we propose different paths of crystallization as a function of chemical diffusion, as shown in Figure 3.

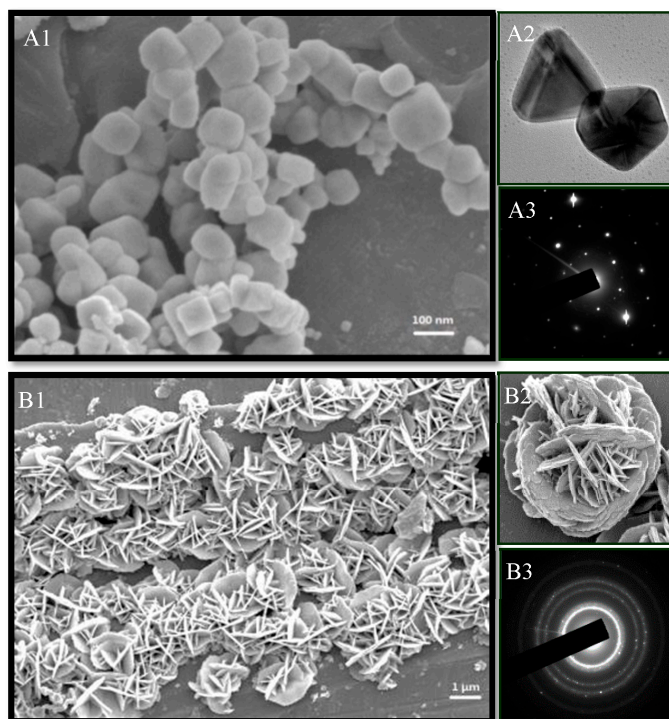


**Figure 1.** Electron micrographs of silver particles synthesized in the mixture of ethanol and water at the ethanol volume ratios of 0.2 (A) and 0.5 (B). (A1,B1) are SEM images of the samples. (A2,B2) are the magnified TEM and SEM images, respectively. (A3,B3) are selected area electron diffraction patterns of the corresponding particles.

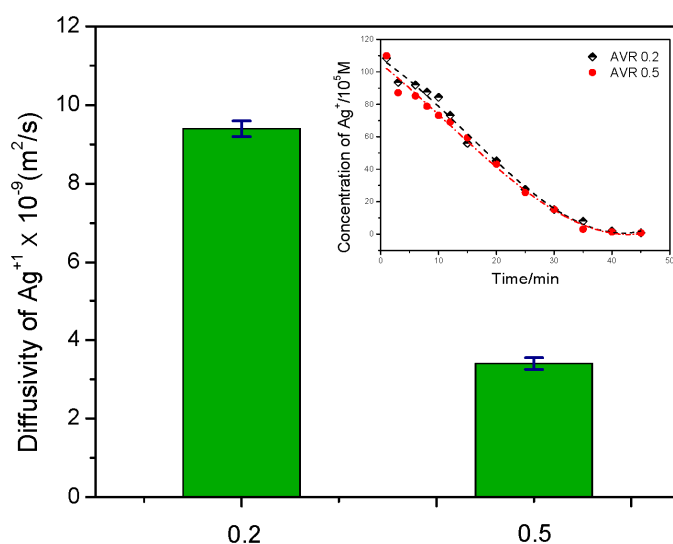


**Figure 2.** Bar graphs show the diffusivities of silver ions at different ethanol volume ratios. The inset shows the time-dependent silver ion concentration during the reaction, indicating the similar reduction rates of silver ions at different ethanol volume ratios.

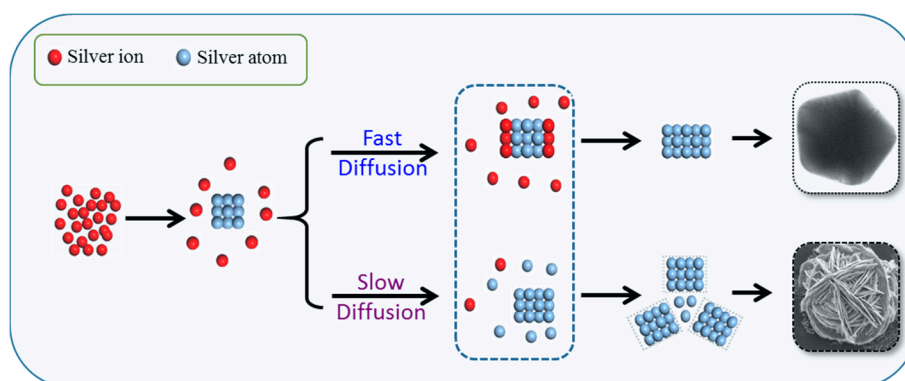


**Figure 3.** Schematic illustration of how diffusion rate of silver ions changes the growth pathways of crystals, leading to the formation of distinct shapes of products.

According to the models proposed in Figure 3, some silver ions are firstly reduced to silver atoms, inducing nucleation. The remaining silver ions participate in the growth of particles by one of two pathways, as determined by the diffusion rate of the silver ions. When the diffusion of silver ions was relatively high (upper layer in Figure 3), the silver ions or their reduction products (atoms) had high mobility, meeting the nuclei where they were incorporated into the lattice, forming small crystals in accordance with the classic layer-wise growth mode [34]. In contrast, when the diffusivity of the silver ions was low, the collision probability between silver ions and the nuclei was lowered. As a result, the remaining silver ions were preferentially reduced to silver atoms in the solution, inducing secondary nucleation. The nuclei are not stable in solution. They tended to aggregate together to reduce the surface energy. But their aggregation was restricted, due to the high viscosity of solvents. When the sample suspensions were dropped on copper substrates, the colloids were compacted to the surface of the substrates, followed by the growth of colloids, resulting in the formation of hierarchical structures.

To confirm the formation process of the hierarchical structures, a suspension of samples synthesized at 50 vol% ethanol was dropped onto different substrates, as shown in Figure 4. When the suspension was dropped onto a copper grid, the water was quickly left out, and silver particles with sizes of less than 10 nm were observed in the grid, as shown in Figure 4A. When the suspension was dropped onto a dense copper foil, the liquid remained on the foil for several hours at room temperature until it was completely dried. Flower-like hierarchical structures were formed on the copper substrate, as shown in Figure 4B. Therefore, the evaporation process is significant for the formation of flower-like particles.

The evaporation had at least two effects. First, it increased the saturation of the solution in the droplets, which induced the growth of silver particles in the droplets. Second, it created a concentration gradient at the surface of the droplets. The outside surface had a high concentration of chemicals, while the inside surface had a low concentration, owing to the evaporation of the solvents [35,36]. Under the concentration gradient, the silver particles aggregated tended to grow towards the surface, forming plate-like particles. The interconnection of the plate-like particles formed flower-like structures. To verify this formation process, we synthesized silver particles at an ethanol volume ratio of 0.5. Then, the suspension was dropped onto copper substrate. The evaporation of the solvent was stopped at different times, and the samples on the substrates were washed with ethanol. Then, the samples were subjected to electron microscopy, as shown in Figure 5. After 1 h evaporation, small dendritic particles were formed, distributed randomly on the substrate, as shown in Figure 5A. With the prolongation of evaporation, the dendrites grew, forming branch-like particles (Figure 5B). Later, these particles formed feather-like plates (Figure 5C). On the edge of the feather particles, fractal structures predominated, indicating growth on the edges. With further prolongation of evaporation, the feather particles interconnected together, forming flower-like particles with rounded outer profiles (Figure 5D). Here, the replacement reaction may have been involved in the formation of silver particles, whereby the

surface of the copper plate was oxidized and the silver ions were reduced at the growth front of the silver plate. When we dropped the suspension onto an alumina substrate, silver aggregates with thick brick-like particles as building blocks were obtained. Therefore, substrates play an important role in the formation of hierarchical structures.

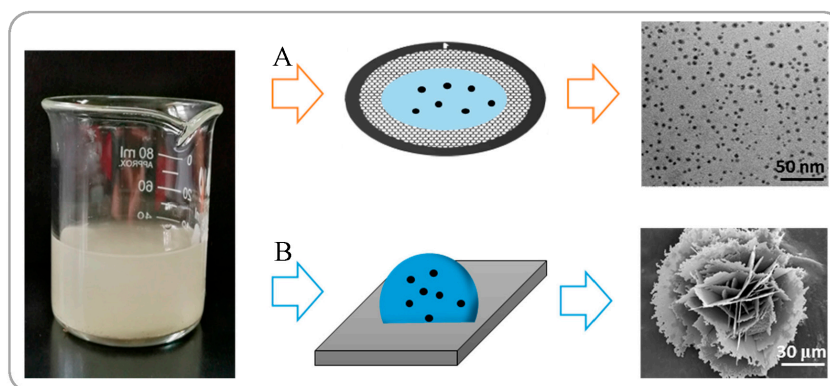


**Figure 4.** Dropping the suspension on different substrates leads to the formation of different morphologies of silver products. (A) When the suspension was dropped on the copper grid, small silver particles with sizes of less than 10 nm were observed; (B) When the suspension was dropped on copper substrates, flower-like particles were observed after evaporation at room temperature.

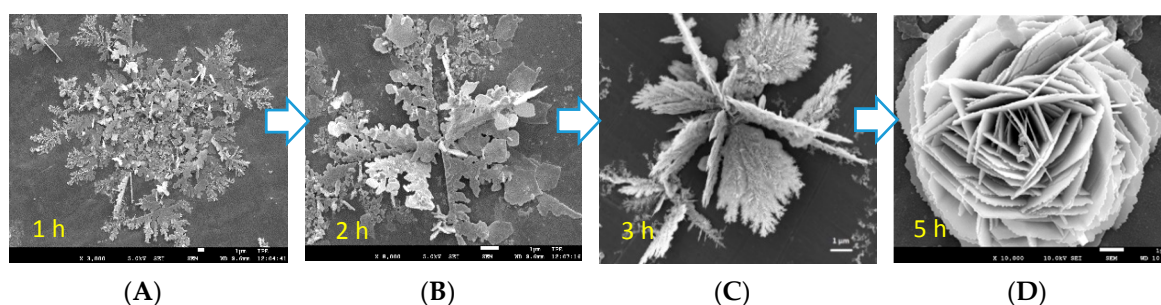


**Figure 5.** The morphology of samples dropped onto copper substrates after different evaporation times (A) 1 h; (B) 2 h; (C) 3 h and (D) 5 h.

For the formation of flower-like particles, silver ions are assumed to have largely been reduced in the solution. Therefore, silver atoms or their clusters should be present in greater numbers in the solution during the reaction. To quantify the silver atoms and clusters in the solution, we designed a setup to separate silver atoms and clusters from the solution. The details of this setup were described in the experimental section. To start with, silvers in the solution were in the form of silver ions, silver atoms, clusters, nuclei and large silver particles. Here, clusters refer to the unstable aggregates of silver atoms that are small enough to pass through the filter. The liquid samples taken from the suspension initially went through the filter, which entrapped the nuclei and large particles of the solution, leaving silver ions, atoms and clusters in the outflow. Then, the outflow was injected into a cation exchange chromatographic column, in which the silver ions were selectively adsorbed in the column via the ion exchange process. Therefore, after these treatments, only silver atoms and clusters remained in the outflow, and these were then subsequently subjected to atomic absorption spectroscopy, as shown in Figure 6. When the reaction was carried out for a low volume ratio of ethanol (20%), approximately 0.2~0.4 ppm silver atoms was detected in the solution. When the reaction took place at a high ethanol volume ratio of (50%), the silver atom concentration reached approximately 1 ppm. Therefore, the amount of silver atoms in the solution increased with the volume ratio of ethanol,

confirming the previous assumption that more silver atoms or clusters are formed in solution under decreased diffusion conditions, thus favoring the coalescence growth model.

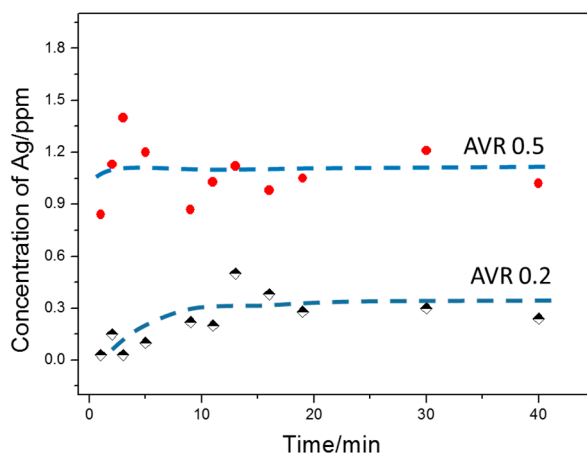


**Figure 6.** Concentration of silver atoms in the solvent changes with the reaction time with different ethanol volume ratios (AVR).

To exclude the chemical effect on the morphologies of silver products, we used propanol to replace ethanol, and synthesized silver particles at different propanol volume ratios. Since the viscosity of propanol is similar to that of ethanol, the diffusivity of silver ions at the same volume ratio was similar to that of ethanol. At the propanol volume ratio of 0.2, smooth crystals were formed, while flower-like hierarchical structures were formed at a volume ratio of 0.5, as shown in the insets of Figure 7A. The morphologies obtained for the propanol solution were similar to those formed in the ethanol solution. This indicates that the change in silver morphology is independent on the type of alcohol. Furthermore, we quantified the atom concentration in the propanol solution, as shown in Figure 7B. At the higher propanol volume ratio of 0.5, the atom concentration was higher than that for the ratio of 0.2, which is in good agreement with the results for the ethanol solution. Therefore, regardless of the alcohol employed, the low diffusivity of silver ions led to a high concentration of silver atoms in the solution, favoring the initial coalescence and subsequent classical growth and formation of hierarchical structures.

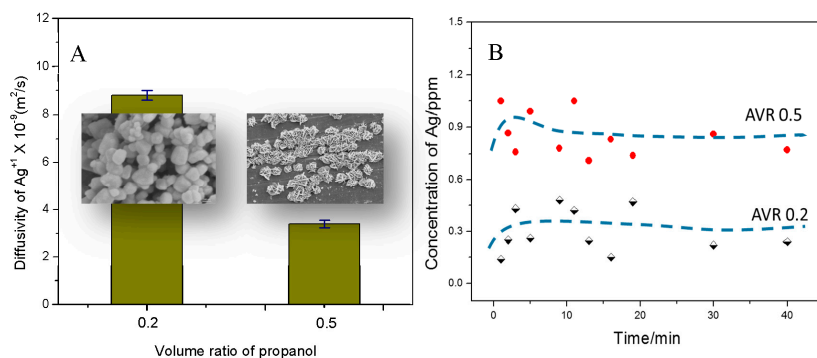


**Figure 7.** Diffusivity of silver ions at different volume ratios of propanol, and the silver morphologies formed in each solvent: (A) Concentration of silver atoms in the solution changes with reaction time at different propanol volume ratios; and (B) AVR means alcohol volume ratio.

### 3. Materials and Methods

#### 3.1. Synthesis of Silver Particles in Different Solvents

Reagents (analytical grade) used in the experiment were purchased from Sigma (Beijing), and purified water with a resistivity higher than 18 mΩ/cm was used. A solution of AgNO<sub>3</sub> (0.1 M) was prepared by dissolving analytically pure AgNO<sub>3</sub> reagent in purified water. A solution of sodium citrate (3.5 mM, 100 mL) was prepared in a flask by dissolving sodium citrate in the mixture of alcohol and water at different alcohol volume ratios (0.2, 0.5). The flask was heated to boiling for 30 min under vigorous stirring. Then AgNO<sub>3</sub> solution was injected into the flask to initiate the reaction. The solution changed color gradually from colorless to yellow, and to turbid. After 50 min, the reaction was stopped and the products were sampled.

#### 3.2. Characterization on the Morphologies of Samples

The shape of samples was examined by a JSM-6700F scanning electron microscope fitted with a field emission source at an accelerating voltage of 20 kV. Samples were spread on double-sided carbon wafer tapes and coated with gold prior to the microscopic characterization. The products were further investigated by transmission electron microscopy (TEM) using a JEM-2100 (UHR) high-resolution transmission microscope at an accelerating voltage of 200 kV.

#### 3.3. Quantification on the Diffusivity of Silver Ions in Different Solvents

The diffusivity of silver ions in alcohol/water mixtures was determined on the basis of the Nernst-Einstein equation:

$$D_i = \frac{RT\lambda_m^\infty t_i}{z^2 F^2} \quad (1)$$

where,  $D_i$  is the diffusivity of species  $i$  (cm<sup>2</sup>/s),  $R$  is the gas constant (8.314 J/(mol·K)),  $T$  is the absolute temperature (K),  $z$  is the charge of species  $i$ ,  $F$  is the Faraday constant (96,500 C/mol),  $\lambda_m^\infty$  is the molar conductivity of all conductive species at infinite dilution, and  $t_i$  is the transference number of species  $i$ . The transference number of Ag<sup>+</sup> in aqueous solution of AgNO<sub>3</sub> is taken as 0.468 [21]. The conductivities of silver salt in the mixture of alcohol and water were measured by a pH/conductivity meter (Mettler-Toledo S470 Seven Excellence, Zurich, Switzerland). On the basis of this measurement, we firstly obtained the molar conductivity [37] of AgNO<sub>3</sub> at different concentrations; then, by extrapolating the conductivity curve to infinite dilute concentration, we obtained the molar conductivity of AgNO<sub>3</sub> at its infinite dilution. Subsequently, it was possible to calculate the diffusivity of silver ions using Equation (1).

#### 3.4. Quantification of Reaction Rate of Silver Ions in Different Solvents

The reduction rate of silver ions was determined by tracking the concentration evolution of silver ions during the reaction. 1 mL of the solution was removed after designated reaction times, and cooled in ice water immediately to stop the reaction. Silver particles were eliminated from the sample by filtering via porous cellulose membranes with pore size of 1–2 nm. Then, the concentration of silver ions in the sample was measured by an ion meter equipped with a silver ion selective electrode (Metrohm, perfect ION™ comb Ag/S<sub>2</sub> Combination Electrode, Zurich, Switzerland).

#### 3.5. Measurement of Free Silver Atoms or Clusters in the Reaction Solution

1 mL solution was taken out from the reactor at designated reaction times, and immediately cooled in ice water to stop the reaction. Before measuring the silver atoms, the solution samples containing silver ions, atoms, clusters, and larger particles was introduced into a filtration setup, as demonstrated in Figure 8. After passing through a filtering device containing porous cellulose membranes, the silver particles in the solution were trapped inside. As a result, only silver ions, atoms,

and clusters were left in the outflow solution. Subsequently, the outflow solution was injected into a cation exchange chromatography column, where the silver ions were selectively detained in the column via the ion-exchange process. Then, the purified water flowed through the column to carry out the silver atoms and clusters. The outflow showed no detectable optical absorption peak in the UV-vis scanning mode, confirming the removal of silver particles from the solution. The removal of silver ions was confirmed by adding ion-selective agents into the outflow, while showing no signal. Then, the concentration of free silver atoms and clusters in the outflow was determined by flame furnace atomic absorption (AA) spectrometry (Varian AA240).

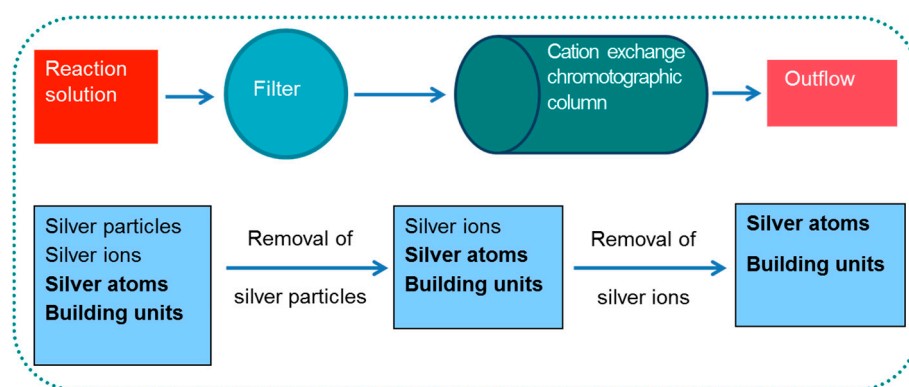


**Figure 8.** Schematic demonstration on the procedure of removing silver particles and silver ions from the reaction solution.

#### 4. Conclusions

This paper investigated the role of chemical diffusion on the shape development of silver particles. At a high diffusivity of silver ions, small cubic silver crystals were generated, while flower-like hierarchical structures were formed at a lower diffusivity. Further investigation indicated that high diffusivities of silver ions favored classic crystallization via discrete nucleation, followed by a layer-wise growth process. At low diffusivity, the movement of silver ions was restricted, and they were liable to be reduced in the solution and stabilized by the solvent. When the suspension was dropped onto a copper substrate, the colloids in the solution were deposited onto the surface of the substrate. Under the evaporation of solvent, the aggregated colloids grew via classic crystallization, forming interconnecting, plate-like units, which generated flower-like structures. This study confirms that chemical diffusivity plays an important role in crystallization, and describes new understanding of the formation of hierarchical structures. Additionally, the synthesized flower particles look like the desert rose stones, which were found in the desert, but formed thousands of years ago. Their formation history and environment are the subject of great conjecture. This study shines light on the formation mechanisms of these beautiful stones [38].

**Acknowledgments:** This study was supported by the National Natural Science Foundation of China (U1462130, No. 21406232) and the State Key Laboratory of Multiphase Complex Systems (MPCS-2014-D-05). Helmuth Moehwald from the Max Planck Institute of Colloids and Interfaces is acknowledged for the fruitful discussions and revisions.

**Author Contributions:** Han Wang and Qiang Lin conceived and designed the experiments; Xiangyu Dou and Tao Yang analyzed the data; Yongsheng Han wrote the paper.

**Conflicts of Interest:** The authors declare no conflict of interest.

#### References

- Porter, N.S.; Wu, H.; Quan, Z.W.; Fang, J.Y. Shape-control and electrocatalytic activity-enhancement of Pt-based bimetallic nanocrystals. *Acc. Chem. Res.* **2013**, *46*, 1867–1877. [[CrossRef](#)] [[PubMed](#)]

2. Khalavka, Y.; Becker, J.; Sonnichsen, C. Synthesis of rod-shaped gold nanorattles with improved plasmon sensitivity and catalytic activity. *J. Am. Chem. Soc.* **2009**, *131*, 1871–1875. [[CrossRef](#)] [[PubMed](#)]
3. Lignier, P.; Bellabarba, R.; Tooze, R.P.; Su, Z.; Landon, P.; Ménard, H.; Zhou, W. Facile synthesis of branched ruthenium nanocrystals and their use in catalysis. *Cryst. Growth Des.* **2011**, *12*, 939–942. [[CrossRef](#)]
4. Boukhalfa, S.; Chaieb, S. Etched Glass self-assembles into micron-size hollow platonic solids. *Cryst. Growth Des.* **2012**, *12*, 4692–4695. [[CrossRef](#)]
5. Shankar, S.S.; Rai, A.; Ankamwar, B.; Singh, A.; Ahmad, A.; Sastry, M. Biological synthesis of triangular gold nanoprisms. *Nat. Mater.* **2004**, *3*, 482–488. [[CrossRef](#)] [[PubMed](#)]
6. Kongkanand, A.; Tvrđy, K.; Takechi, K.; Kuno, M.; Kamat, P.V. Quantum dot solar cells. Tuning photoresponse through size and shape control of CdSe-TiO<sub>2</sub> architecture. *J. Am. Chem. Soc.* **2008**, *130*, 4007–4015. [[CrossRef](#)] [[PubMed](#)]
7. Ithurria, S.; Tessier, M.; Mahler, B.; Lobo, R.; Dubertret, B.; Efros, A.L. Colloidal nanoplatelets with two-dimensional electronic structure. *Nat. Mater.* **2011**, *10*, 936–941. [[CrossRef](#)] [[PubMed](#)]
8. Wiley, B.J.; Im, S.H.; Li, Z.-Y.; McLellan, J.; Siekkinen, A.; Xia, Y. Maneuvering the surface plasmon resonance of silver nanostructures through shape-controlled synthesis. *J. Phys. Chem. B* **2006**, *110*, 15666–15675. [[CrossRef](#)] [[PubMed](#)]
9. Alivisatos, P. The use of nanocrystals in biological detection. *Nat. Biotechnol.* **2004**, *22*, 47–52. [[CrossRef](#)] [[PubMed](#)]
10. Anker, J.N.; Hall, W.P.; Lyandres, O.; Shah, N.C.; Zhao, J.; Van Duyne, R.P. Biosensing with plasmonic nanosensors. *Nat. Mater.* **2008**, *7*, 442–453. [[CrossRef](#)] [[PubMed](#)]
11. Li, J.; Ge, W.; Wang, W.; Yang, N.; Liu, X.; Wang, L.; He, X.; Wang, X.; Wang, J.; Kwauk, M. *From Multiscale Modeling to Meso-Science*; Springer: Berlin, Germany, 2013.
12. Chen, G.; Cheng, H.; Zhang, W.; Yang, Z.; Qiu, M.; Zhu, X.; Chen, M. Template-free synthesis of single-/double-walled TiO<sub>2</sub> nanovesicles: Potential photocatalysts for engineering application. *AIChE J.* **2015**, *61*, 1478–1482. [[CrossRef](#)]
13. Tian, G.L.; Zhang, Q.; Zhao, M.Q.; Wang, H.F.; Chen, C.M.; Wei, F. Fluidized-bed CVD of unstacked double-layer templated graphene and its application in supercapacitors. *AIChE J.* **2015**, *61*, 747–755. [[CrossRef](#)]
14. Aziz, B.; Gebauer, D.; Hedin, N. Kinetic control of particle-mediated calcium carbonate crystallization. *CrystEngComm* **2011**, *13*, 4641–4645. [[CrossRef](#)]
15. Martinolich, A.J.; Kurzman, J.A.; Neilson, J.R. Polymorph selectivity of superconducting CuSe<sub>2</sub> through kinetic control of solid-state metathesis. *J. Am. Chem. Soc.* **2015**, *137*, 3827–3833. [[CrossRef](#)] [[PubMed](#)]
16. Horst, J.H.; Geertman, R.M.; van Rosmalen, G.M. The effect of solvent on crystal morphology. *J. Cryst. Growth* **2001**, *230*, 277–284. [[CrossRef](#)]
17. Meng, X.K.; Tang, S.C.; Vongehr, S. A review on diverse silver nanostructures. *J. Mater. Sci. Technol.* **2010**, *26*, 487–522. [[CrossRef](#)]
18. Ouyang, J.J.; Pei, J.; Kuang, Q.; Xie, Z.X.; Zheng, L.S. Supersaturation-controlled shape evolution of alpha-Fe<sub>2</sub>O<sub>3</sub> nanocrystals and their facet-dependent catalytic and sensing properties. *ACS Appl. Mater. Interfaces* **2014**, *6*, 12505–12514. [[CrossRef](#)] [[PubMed](#)]
19. Lee, S.-H.; Koo, M.-J.; Jazbinsek, M.; Kwon, O.P. Origin of solubility behavior of polar pi-conjugated crystals in mixed solvent systems. *Cryst. Growth Des.* **2014**, *14*, 6024–6032. [[CrossRef](#)]
20. Eddleston, M.D.; Hejczyk, K.E.; Cassidy, A.M.C.; Thompson, H.P.G.; Day, G.M.; Jones, W. Highly unusual triangular crystals of theophylline: The influence of solvent on the growth rates of polar crystal faces. *Cryst. Growth Des.* **2015**, *15*, 2514–2523. [[CrossRef](#)]
21. Xia, X.H.; Figueroa-Cosme, L.; Tao, J.; Peng, H.C.; Niu, G.D.; Zhu, Y.M.; Xia, Y.N. Facile Synthesis of iridium nanocrystals with well-controlled facets using seed-mediated growth. *J. Am. Chem. Soc.* **2014**, *136*, 10878–10881. [[CrossRef](#)] [[PubMed](#)]
22. Darby, B.L.; Le Ru, E.C. Competition between molecular adsorption and diffusion: Dramatic consequences for SERS in colloidal solutions. *J. Am. Chem. Soc.* **2014**, *136*, 10965–10973. [[CrossRef](#)] [[PubMed](#)]
23. Witten, T.A.; Sander, L.M. Diffusion-limited aggregation, a kinetic critical phenomenon. *Phys. Rev. Lett.* **1981**, *47*, 1400–1403. [[CrossRef](#)]
24. Wang, H.; Han, Y.S.; Li, J.H. Dominant role of compromise between diffusion and reaction in the formation of snow-shaped vaterite. *Cryst. Growth Des.* **2013**, *13*, 1820–1825. [[CrossRef](#)]

25. Yang, Y.; Wang, H.; Ji, Z.; Han, Y.S.; Li, J.H. A switch from classic crystallization to non-classic crystallization by controlling the diffusion of chemicals. *CrystEngComm* **2014**, *16*, 7633–7637. [[CrossRef](#)]
26. Lamer, V.K.; Dinegar, R.H. Theory, production and mechanism of formation of monodispersed hydrosols. *J. Am. Chem. Soc.* **1950**, *72*, 4847–4854. [[CrossRef](#)]
27. Reiss, H. The growth of uniform colloidal dispersions. *J. Chem. Phys.* **1951**, *19*, 482–487. [[CrossRef](#)]
28. Peng, X.G.; Wickham, J.; Alivisatos, A.P. Kinetics of II-VI and III-V colloidal semiconductor nanocrystal growth: “focusing” of size distributions. *J. Am. Chem. Soc.* **1998**, *120*, 5343–5344. [[CrossRef](#)]
29. Murray, C.B.; Kagan, C.R.; Bawendi, M.G. Synthesis and characterization of monodisperse nanocrystals and close-packed nanocrystal assemblies. *Annu. Rev. Mater. Sci.* **2000**, *30*, 545–610. [[CrossRef](#)]
30. Niederberger, M.; Colfen, H. Oriented attachment and mesocrystals: Non-classical crystallization mechanisms based on nanoparticle assembly. *Phys. Chem. Chem. Phys.* **2006**, *8*, 3271–3287. [[CrossRef](#)] [[PubMed](#)]
31. Banfield, J.F.; Welch, S.A.; Zhang, H.Z.; Ebert, T.T.; Penn, R.L. Aggregation-based crystal growth and microstructure development in natural iron oxyhydroxide biomineralization products. *Science* **2000**, *289*, 751–754. [[CrossRef](#)] [[PubMed](#)]
32. Zheng, H.M.; Smith, R.K.; Jun, Y.W.; Kisielowski, C.; Dahmen, U.; Alivisatos, A.P. Observation of single colloidal platinum nanocrystal growth trajectories. *Science* **2009**, *324*, 1309–1312. [[CrossRef](#)] [[PubMed](#)]
33. Li, Z.Q.; Tao, J.; Lu, X.M.; Zhu, Y.M.; Xia, Y.N. Facile synthesis of ultrathin Au nanorods by aging the AuCl(oleylamine) complex with amorphous Fe nanoparticles in chloroform. *Nano Lett.* **2008**, *8*, 3052–3055. [[CrossRef](#)] [[PubMed](#)]
34. Xia, X.H.; Zeng, J.; Oetjen, L.K.; Li, Q.G.; Xia, Y.N. Quantitative analysis of the role played by poly(vinylpyrrolidone) in seed-mediated growth of Ag nanocrystals. *J. Am. Chem. Soc.* **2012**, *134*, 1793–1801. [[CrossRef](#)] [[PubMed](#)]
35. Shokri, N.; Lehmann, P.; Or, D. Liquid-phase continuity and solute concentration dynamics during evaporation from porous media: Pore-scale processes near vaporization surface. *Phys. Rev. E* **2010**, *81*, 046308. [[CrossRef](#)] [[PubMed](#)]
36. Huang, S.; Li, H.; Wen, H.; Yu, D.; Jiang, S.; Li, G.; Chen, X.; An, L. Solvent micro-evaporation and concentration gradient synergistically induced crystallization of poly(L-lactide) and ring banded supra-structures with radial periodic variation of thickness. *CrystEngComm* **2014**, *16*, 94–101. [[CrossRef](#)]
37. Bishop, A.G.; MacFarlane, D.R.; Forsyth, M. Ion association and molar conductivity in polyether electrolytes. *Electrochim. Acta* **1998**, *43*, 1453–1457. [[CrossRef](#)]
38. Wang, M.; Bao, W.J.; Wang, J.; Wang, K.; Xu, J.J.; Chen, H.Y.; Xia, X.H. A green approach to the synthesis of novel “desert rose stone”-like nanobiocatalytic system with excellent enzyme activity and stability. *Sci. Rep.* **2014**, *4*, 6606. [[CrossRef](#)] [[PubMed](#)]

